DISCLAIMER

Nanowire-based Single Cell Endoscopy

Ruoxue Yan[1†], Ji-Ho Park[1,2†], Yeonho Choi[3,4], Chul-Joon Heo[3,5], Seung-Man Yang[5], Luke P. Lee[3], and Peidong Yang[1]*

[1]Department of Chemistry, University of California, and Materials Sciences Division, Lawrence Berkeley National Laboratory, Berkeley, California 94720, USA

[2]Department of Bio and Brain Engineering, Korea Advanced Institute of Science and Technology, Daejeon 305-701, South Korea

[3]Department of Bioengineering, University of California, Berkeley, California 94720, USA

[4]Department of Biomedical Engineering, Korea University, Seoul, 136-703, South Korea

[5]CRI Center for Integrated Optofluidic Systems, Department of Chemical and Biomolecular Engineering, Korea Advanced Institute of Science and Technology, Daejeon, 305-701, South Korea

[†]These authors contributed equally to this work.

*e-mail: p_yang@uclink.berkeley.edu

Keywords: biological imaging, biological sensing, payload delivery, semiconductor nanowire, endoscopy

One dimensional smart probes based on nanowires and nanotubes that can safely penetrate the plasma membrane into biological cells hold enormous potential in high resolution[1-6] and high throughput[7,8] gene and drug delivery, biosensing[6,9] and single cell electrophysiology[6,10]. However, the efforts to use them for optical communication cross the cellular membrane at the subwavelength level remains very limited. Here, we show that a nanowire waveguide attached to the tapered tip of an optical fibre can guide visible light into intracellular compartments of a living mammalian cell, and detect optical signals from subcellular regions with high spatial resolution. Furthermore, we show that the endoscope is capable of delivering payloads through light activated release mechanism into cells with spatiotemporal specificity. Moreover, insertion of the endoscope into cells and illumination of the guided laser did not induce any significant toxicity in the cells.

Optical nanoscopy, a high resolution technique that breaks the diffraction barrier, has been recently introduced to study chemistry, biology, and physics in intracellular molecular processes[11-13]. Although current optical techniques have now reached the subcellular level, high-precision optical imaging systems are complex, expensive, and bulky. Therefore, incorporating nanophotonic component into simple, low-cost, bench-top optical setups would miniaturize spectroscopic analyses, and are particularly useful for studying chemical and biological events inside single cells and their substructures. Fluorescence sensing techniques based on submicron tapered optical fibres have been developed for probing living biological specimen[14-17], but the large and conical shaped fibres mean that their illumination volume remains large and they can easily rupture cellular membranes. Nevertheless, fibre-optic fluorescence imaging techniques have unique features that can be incorporated into handheld optical systems and flexible endoscopes for minimally invasive imaging of opaque biological specimens such as tissues[18]. Integrating nanophotonic probes into the fibre-optic imaging system allow us to manipulate light at the nanoscale inside living cells for studying photo-active biological processes[19,20] and for bioanalytical analyses[21,22].

Previously, we showed that subwavelength dielectric nanowire waveguides can efficiently shuttle ultraviolet and visible light in air and fluidic media[23,24]. The nanowires are promising for interrogating intracellular environments because their small dimension (100~250 nm) and mechanical flexibility minimize their damage to cellular structures and functions. Furthermore, because of their higher refractive index (n = 2.1~2.2) than that of the conventional optical fibre (n = ~1.5), the nanowires can guide visible light efficiently in high-index physiological liquids and living cells (n = 1.3~1.5). In addition, the oxide surface of nanowires can be readily functionalized, enabling payload delivery and specific sensing inside the cell. Recently, there have been increasing efforts in interfacing nanowire arrays with living cells to modulate physicochemical properties of the cell and deliver biomolecules into the subcellular environments[25-27]. By controlling nanowire diameter, length and density, they can be safely internalized into the cell without disturbing cell proliferation and differentiation.

Here, combining the advantages of nanowire waveguides and fibre-optic fluorescence imaging technique, we designed a novel nanowire-based endoscope system (Figure 1a) for optical probing inside single cells and spatiotemporally deliver payloads into intracellular sites with minimal perturbation to the cellular system.

The nanowire endoscope was fabricated by bonding a SnO_2 nanowire to the tapered tip of an optical fibre (Figure S1-2). Light traveling along the optical fibre can be effectively coupled into the nanowire and travel to nanowire tip where it is re-emitted to the free-space (Figure 1b). Mechanical stability is a fundamental requirement for biological probes for intracellular sensing and imaging. The nanowire endoscope is extremely flexible due to its small size and high aspect ratio, yet is very robust mechanically, and can endure repeated deformation, bending and buckling without being peeled off from the fibre. Figure

1d shows that under a 20º deformation, the nanowire remains firmly attached to the fibre tip, and the intensity of its tip emission did not show significant fall-off compared to that when it's free of mechanical deformation (Figure 1c), indicating that the optical coupling also remained undisturbed.

Highly efficient optical coupling between the nanowire and the optical fibre is crucial for the nanowire endoscopes to function as localized light sources. To test the waveguiding capability of the nanowire endoscope in physiological environment and to visualize the intensity distribution of the endoscope emission, the endoscope was immersed in cell culture media, which contains fluorescent proteins that can be excited by the endoscope (Figure 1e). The profile of fluorescence intensity follows that of the endoscope emission (Figure 1 f and g). For a highly efficient nanowire endoscope, the optical output is closely confined to the nanowire tip, offering highly directional and localized illumination. Despite the small dimensions of the nanowires, the large increase (~33%) in environmental refractive index did not affect the optical coupling or light propagation, benefiting from the high refractive index of SnO_2.

One important advantage of using nanowires instead of tapered fibre optics for single-cell endoscopy is their low invasiveness resulting from fine diameters and the uniform geometry. As previously demonstrated for silicon and gallium Phosphide nanowire arrays[25-27], nanowires can penetrate the lipid membrane without damaging cellular functions. In order to study the biocompatibility of SnO_2 based nanowire endoscopes, cell viability, apoptosis, intracellular stress and membrane integrity tests were performed to evaluate the impact of the nanowire insertion process at single-cell level. We found that the nanowire insertion into the cytoplasm did not induce cell death (Table S1, Figure S5), apoptosis (Figure S6), significant cellular stress (Figure S7, Video S2) or membrane rupture (Figure S8) for the experimental conditions required for the subsequent spot cargo delivery and endoscopy studies. In contrast, the insertion of tapered optical fibre tip caused the demise of 40% of the plated cells, and also induced considerable cellular stress and cell membrane rupture (Supplementary Section II). Moreover, the nanoprobe illumination on the intracellular environment of HeLa cell with waveguided blue light was also proven to be harmless due to the small illumination volume (down to picoliter) (Table S2).

Having demonstrated the biocompatibility of the nanowire endoscope, the feasibility of delivering payloads into specific intracellular sites with functionalized endoscopes was investigated next. Carbon and boron nitride nanotube-based delivery systems have been reported previously[1,28], where payloads (e.g. QDs) were attached to the nanotube via disulfide bond linkers which were cleavable in the reducing environment of the cytoplasm. A major limitation for this passive delivery system is the long insertion time (20-30 mins) and the lack of temporal control over the delivery process (Figure S9). To reduce insertion time and improve temporal control, we used photo-cleavable linkers (Figure 2a), which can be cleaved by low power UV radiation in 1 min. QDs can be selectively coupled to the nanowire tip through the photo-cleavable linker (Figure 2b-c) and the functionalized endoscope can release QDs into intended intracellular sites

(Figure 2d-e) within 1 min of simultaneous nanowire insertion and UV laser illumination focused on the nanowire tip. The intracellular delivery of QDs through this light-activated mechanism was confirmed by cellular confocal scan after QD delivery, which clearly showed the QDs residing within the cytoplasm encompassed by fluorescently labeled membrane (Figure 2f). The photo-activation at this level had no significant effects on cell viability (Table S2). The QD delivery set up could be further integrated by fabricating the nanowire endoscope with a UV transparent optical fibre, so that the required UV excitation can be delivered directly through the nanowire.

The nanowire endoscope illumination is capable of high resolution and high contrast subcellular imaging and tracking of fluorescent species (Figure 3a). The illumination resolution was first studied with QDs, which have high fluorescence efficiency in cellular environment. Highly directional laser beam from the nanoprobe was able to selectively illuminate one of the two QD clusters spaced merely 2μm apart (Figure 3b and 3c). Intracellular fluorescent molecules, which are far less bright than QDs, can also be locally excited (Figure 3d-f and Figure S12-14). Because of the small illumination area (down to picoliter) and the small separation that can be achieved between the light source and the fluorescent molecules, the endoscope illumination also ensures low background fluorescence and high imaging contrast. Figure 3d shows the fluorescence image of a Hela cell stained with a fluorescent label that binds specifically the cell membrane. Under such wide field illumination, which is typical for epi-fluorescence microscopy, the whole cell membrane, both the top and bottom surfaces, were excited due to the large illumination depth. As a result, out of focus fluorescence would enter the focal plane of the objective and obscure the details of the in-focus image[29]. With much smaller illumination depth, the nanowire endoscope can excite tiny areas on the cellular membrane with much lower background. Figure 3e-f demonstrated the spot illumination ability when the nanowire approached the cell membrane from the side and Figure S14 further shows that it is possible to distinguish the fluorescence signals from the top and the bottom of the cell membrane with the highly localized endoscope illumination. The high spatial resolution imaging capability of the nanowire endoscope was not achieved by sacrificing its temporal resolution. The nanowire endoscope can also be used for subcellular fluorescence tracking (Figure S15) and holds potentials for sensing molecular kinetics in intracellular substructures (e.g. mitochondria).

A pH-sensitive endoscope were also fabricated by coating the nanowire tip with a polymer embedded with pH-sensitive dyes (Figure 4a-e) and preliminarily tests demonstrated the potential of sensing pH change in the submicron environment using the functionalized nanowire endoscope. By immersing the tip of the pH-sensitive endoscope into micro-droplets (<10 pL in volume) of buffer solutions of different pH values, it was able to report pH-dependent fluorescence with the excitation of the endoscope tip emission and a calibration curve with a sharp transition between pH 5-9 was established (Figure 4f-g).

An inverse process of waveguided illumination from the tip of the nanowire endoscope, the collection of fluorescent signal from subcellular region through the endoscope was also demonstrated. As illustrated in Figure 5a-c, the fluorescence spectra of a single QD cluster in the cytoplasm was collected by the tip of a nanowire endoscope placed next to the cluster. The signal collection was very sensitive to the distance between the QD cluster and the nanowire tip (Figure 5d-e), opening up the possibility for high spatial resolution fluorescence mapping and probing of the interior of non-transparent living biological objects, which would be impossible for bulky near-field scanning optical microscope tips.

In conclusion, we have developed a versatile and biocompatible nanowire-based optical probe for intracellular cargo delivery with high spatiotemporal precision and endoscopy with high spatial and temporal resolution. These nanowire endoscopes are highly flexible and robust, both mechanically and optically, and can endure repeated bending and deformation during cell imaging process. The effective optical coupling between the fibre optics and the nanowire enables highly localized excitation and detection, limiting the probe volume to the close proximity of the nanowire, making it a promising candidate for high resolution optical imaging, mapping and chemical/biological sensing along with the precision delivery of gene, proteins, and drugs.

Methods

SnO_2 Nanowire Synthesis.

The experimental procedure is described in the Supplementary Information.

Optical Fibre Etching.

The experimental procedure is described in the Supplementary Information.

Nanowire endoscope Fabrication.

The fabrication procedure of the nanowire endoscope is illustrated by the schematics in Figure S1. First, a SnO_2 nanowire (100-250nm) was picked up from the substrate with a motorized 3-axis micromanipulator (spatial resolution: 100 nm/step) and put on top of the tapered tip of a chemically etched single mode optical fibre with a cone angle of 3-5º and tip diameter of 300-500 nm (S405-HP and 630-HP, Thorlabs Inc.). The relative position of the nanowire and fibre tip was adjusted to minimize the scattering loss at the ribbon-fibre junction. Then a droplet of premixed epoxy glue (ITW Devcon) or Polydimethylsiloxane (Sylgard® 184 Silicone Elastomer, Dow-Corning) was applied to the overlapping nanowire-fibre junction with the micromanipulator needle to bond them permanently.

QD Conjugation onto SnO_2 Nanowire.

The experimental procedure is described in the Supplementary Information.

Optical Setup.

All experiments reported in this work were performed on an upright dark-field optical microscope (Nikon Inc., Melville, NY). A HeCd laser (Melles Griot, Irvine, CA) supplied unpolarized continuous wave (CW) UV excitation (325nm) to the photo-cleavable linkers and 442 nm visible excitation for QD fluorescence. The lasers were focused either directly on the cell at a ~20º glancing angle with the focal plane of the microscope objective lens, or on the tip of the optical fibre mounted on a 5-axis single mode optical fibre coupler (Newport Corporation). A 650nm CW diode laser (Thorlabs Inc., Newton, NJ) was used to test the nanowire endoscope coupling for 630HP fibres. Dark field and fluorescent images were collected through 20x (NA=0.40) and 50x (NA=0.55) long working distance objectives and recorded with a microscope-mounted camera (iXon, Andor Technology, Belfast, Northern Ireland). Spectra were acquired by connecting the optical fibre to a UV-Vis spectrometer (gratings at 1,200 grooves per mm, SpecraPro 300i, Roper Scientific, Trenton, NJ) and liquid N_2-cooled charge-coupled device setup. A 532nm long pass filter was always used for fluorescence imaging.

Payload Delivery Experiment.

HeLa cells were seeded into 35 mm petri-dish with grids and cultured overnight (22,000 cells per dish) at 37^{o}C in the presence of 10% FBS. The QD-conjugated photoactive nanowire endoscope mounted on the micromanipulator was slowly inserted into the nucleus or cytoplasm. The insertion region was immediately irradiated with the focused 325 nm HeCd laser at 0.4 mW/cm^2 for 1 min, and then the probe was removed from the cell. The fluorescence of QDs translocated into the cell was imaged under 442 nm laser excitation. For confocal imaging, Hela cells were seeded into 35mm glass bottom petri-dish with grids following the same procedure mentioned above. Cells were random chosen from the grid cell culture dish for light activated QD delivery with the nanowire endoscope and the positions of the cells operated on were documented for relocation. Cells were then fixed with 4% paraformaldehyde, stained with Alexa Fluor® 488 conjugate of wheat germ agglutinin (WGA, Invitrogen) and kept in Hank's Balanced Salt Solution (HBSS) for imaging. Confocal image was collected with Zeiss 710 Inverted Laser Scanning Confocal Microscope with 40x oil immersed objective and 488 nm laser excitation.

Subcellular Imaging Experiment.

HeLa cells were seeded into 35 mm petri-dish with grids and cultured overnight (22,000 cells per dish) at 37^{o}C in the presence of 10% FBS. For subcellular QD imaging, two QD clusters were pre-delivered to adjacent spots (~2 μm apart) in the cytoplasm with photoactive nanowire endoscopes. An unmodified nanowire endoscope was placed close to the two QD clusters without direct contact with the cell membrane. The nanowire endoscope was mounted on the micromanipulator to offer precision control over the nanowire endoscope position. The distal end of the optical fibre was coupled to 442nm blue HeCd laser with an input power of 0.4mW through a single mode fibre coupler. For the cell membrane illumination, Hela cells were pre-treated with Alexa Fluor® 488 conjugate of WGA and kept in HBSS for imaging.

Local Collection Experiment.

HeLa cells were seeded into 35 mm petri-dish with grids and cultured overnight (22,000 cells per dish) at 37^{o}C in the presence of 10% FBS. The cells were pre-treated with aminated QDs for 1 hr and rinsed several times with PBS. QD fluorescence was excited by focused 442 nm blue laser. The nanowire endoscope was placed close to the QDs in the cytoplasm to pick up local fluorescent signal. The distal end of the optical fibre was connected to a UV-Vis spectrometer and the gratings were calibrated with 442nm and 650nm laser lines. The location of the nanowire endoscope was precisely controlled using the micromanipulator during the experiment.

Author Contributions

R.Y., J.P., Y. C., L.P.L., and P.Y. conceived and designed the research. C.H., Y.C., and S.Y. prepared cell samples and performed the Calcein live cell essay after cytotoxicity tests. R.Y., J.P., and Y. C. performed the experiments. R.X., J.P., Y.C., L.P. L. and P.Y. analyzed the data. R.Y., J.P. and P.Y. wrote the manuscript.

Additional information

Supplementary information accompanies this paper at www.nature.com/naturenanotechnology. Reprints and permission information is available online at http://npg.nature.com/reprintsandpermissions/.

Correspondence and requests for materials should be addressed to P.Y.

References

1 Chen, X., Kis, A., Zettl, A. & Bertozzi, C.R. A cell nanoinjector based on carbon nanotubes. *Proc. Natl. Acad. Sci. USA* **104**, 8218-8222 (2007).

2 Han, S.W. *et al.* A molecular delivery system by using AFM and nanoneedle. *Biosens. Bioelectron.* **20**, 2120-2125 (2005).

3 Han, S.W. *et al.* Gene expression using an ultrathin needle enabling accurate displacement and low invasiveness. *Biochem. Bioph. Res. Co.* **332**, 633-639 (2005).

4 Yum, K., Wang, N. & Yu, M.F. Electrochemically controlled deconjugation and delivery of single quantum dots into the nucleus of living cells. *Small* **6**, 2109-2113 (2010).

5 Yum, K. *et al.* Mechanochemical delivery and dynamic tracking of fluorescent quantum dots in the cytoplasm and nucleus of living cells. *Nano. Lett.* **9**, 2193-2198 (2009).

6 Singhal, R. *et al.* Multifunctional carbon-nanotube cellular endoscopes. *Nature Nanotech.* **6**, 57-64 (2011).

7 Cai, D. *et al.* Highly efficient molecular delivery into mammalian cells using carbon nanotube spearing. *Nat. Methods* **2**, 449-454 (2005).

8 Shalek, A.K. *et al.* Vertical silicon nanowires as a universal platform for delivering biomolecules into living cells. *Proc. Natl. Acad. Sci. USA* **107**, 1870-1875 (2010).

9 Niu, J.J., Schrlau, M.G., Friedman, G. & Gogotsi, Y. Carbon nanotube-tipped endoscope for in situ intracellular surface-enhanced Raman spectroscopy. *Small* **7**, 540-545 (2011).

10 Schrlau, M.G., Dun, N.J. & Bau, H.H. Cell electrophysiology with carbon nanopipettes. *ACS Nano* **3**, 563-568 (2009).

11 Hell, S.W. Far-field optical nanoscopy. *Science* **316**, 1153-1158 (2007).

12 Eggeling, C. *et al.* Direct observation of the nanoscale dynamics of membrane lipids in a living cell. *Nature* **457**, 1159-1162 (2009).

13 Zhuang, X. Nano-imaging with STORM. *Nature Photon.* **3**, 365-367 (2009).
14 Tan, W. *et al.* Submicrometer intracellular chemical optical fiber sensors. *Science* **258**, 778-781 (1992).
15 Vo-Dinh, T., Alarie, J.-P., Cullum, B.M. & Griffin, G.D. Antibody-based nanoprobe for measurement of a fluorescent analyte in a single cell. *Nat. Biotechnol.* **18**, 764-767 (2000).
16 Kasili, P.M., Song, J.M. & Vo-Dinh, T. Optical sensor for the detection of Caspase-9 activity in a single cell. *J. Am. Chem. Soc.* **126**, 2799-2806 (2004).
17 Vo-Dinh, T. & Kasili, P. Fiber-optic nanosensors for single-cell monitoring. *Anal. Bioanal. Chem.* **382**, 918-925 (2005).
18 Flusberg, B.A. *et al.* Fiber-optic fluorescence imaging. *Nat. Methods* **2**, 941-950 (2005).
19 Wu, Y.I. *et al.* A genetically encoded photoactivatable Rac controls the motility of living cells. *Nature* **461**, 104-108 (2009).
20 Andrasfalvy, B.K., Zemelman, B.V., Tang, J.Y. & Vaziri, A. Two-photon single-cell optogenetic control of neuronal activity by sculpted light. *Proc. Natl. Acad. Sci. USA* **107**, 11981-11986 (2010).
21 Lippincott-Schwartz, J. & Patterson, G.H. Development and use of fluorescent protein markers in living cells. *Science* **300**, 87-91 (2003).
22 Bulina, M.E. *et al.* A genetically encoded photosensitizer. *Nat. Biotechnol.* **24**, 95-99 (2006).
23 Law, M. *et al.* Nanoribbon waveguides for subwavelength photonics integration. *Science* **305**, 1269-1273 (2004).
24 Sirbuly, D.J. *et al.* Optical routing and sensing with nanowire assemblies. *Proc. Natl Acad. Sci. USA* **102**, 7800-7805 (2005).
25 Kim, W. *et al.* Interfacing silicon nanowires with mammalian cells. *J. Am. Chem. Soc.* **129**, 7228-7229 (2007).
26 Hallstrom, W. *et al.* Gallium phosphide nanowires as a substrate for cultured neurons. *Nano. Lett.* **7**, 2960-2965 (2007).
27 Shalek, A.K. *et al.* Vertical silicon nanowires as a universal platform for delivering biomolecules into living cells. *Proc. Natl Acad. Sci. USA* **107**, 1870-1875 (2010).
28 Yum, K. *et al.* Mechanochemical delivery and dynamic tracking of fluorescent quantum dots in the cytoplasm and nucleus of living cells. *Nano. Lett.* **9**, 2193-2198 (2009).
29 Conchello, J.A. & Lichtman, J.W. Optical sectioning microscopy. *Nat. Methods* **2**, 920-931 (2005).
30 Pan, Z.W., Dai, Z.R. & Wang, Z.L. Nanobelts of semiconducting oxides. *Science* **291**, 1947-1949 (2001).
31 Haber, L.H., Schaller, R.D., Johnson, J.C. & Saykally, R.J. Shape control of near-field probes using dynamic meniscus etching. *J. Microsc.* **214**, 27-35 (2004).

Acknowledgements

This work was supported by the National Institutes of Health through grant number R21 EB007474-03. We thank Z. Huo for transmission electron microscope observations, D. Sirbuly for the nanowire endoscope bending video, H.E. Jeong, J.W. Lee and Q. Pan for cell culturing, Q. Pan and S. Gweon for discussion.

Figure 1| Design of nanowire-based optical probe for single cell endoscopy. a, Schematic illustration of the nanowire-based cell endoscope system. The nanowire endoscope, consisting of a nanowire waveguide fixed on the tapered tip of an optical fibre, can be inserted into a single living cell at designated positions through a 3-axis micro-manipulating system for spot delivery of payloads. The nanowire endoscope can be optically coupled to either an excitation laser to function as a local light source for subcellular imaging, or a spectrometer to collect local optical signals. **b,** 3D schematic showing blue laser waveguided through a nanowire endoscope constructed by gluing a SnO_2 nanowire to the tip of a tapered single mode optical fibre. **c and d,** Dark field images of an endoscope, which was coupled to a 442 nm blue laser, before (**c**) and during (**d**) deformation by a tungsten needle show the nanowire endoscope is flexible and robust. The yellow arrows in (**b-d**) points to the nanowire tip where the waveguided light was emitted into free space. **e-g,** Intensity profile of the nanowire endoscope emission. Schematic drawing (**d**), dark field (**f**) and fluorescent (**g**) images of a nanowire endoscope immersed in cell culture medium that illuminated fluorescent proteins with the blue light emitted from the nanowire tip. (**f-g**) are the top view of a real nanowire endoscope device illustrated in (**e**). A 442 nm long-pass filter was applied to remove the excitation beam from the fluorescence image (**g**). Scale bars in (**d**) and (**g**): 50 μm.

Figure 2 | Spatiotemporal delivery of quantum dots (QDs) into a single living HeLa cell. a, Schematic of the spatiotemporal delivery of QDs into a living cell using a photoactivable nanowire endoscope. Inset shows QDs were conjugated to the nanowire via photocleavable linkers. **b,** Photoluminescence spectrum of the QD (em. 655 nm)-conjugated SnO_2 nanowire endoscope. The nanowire-QD region on the endoscope was directly excited with a focused HeCd laser (325 nm). Inset: Transmission electron microscope (TEM) image of the QD-conjugated SnO_2 nanoprobe. Nanowires with smaller sizes than average nanowire endoscopes were selected for TEM imaging for better contrast. **c,** Dark-field (left panel) and fluorescence (right panel) images of the QD-conjugated SnO_2 nanowire endoscope. **d,** Dark-field image showing a nanowire endoscope inserted into the cell nucleus (left panel). Fluorescence image taken after focused UV irradiation (325 nm, 1 min) on the nanoprobe tip, showing the QD fluorescence in the cell nucleus region under 442 nm laser excitation (right panel). Dark field illumination was left on when the fluorescent image was captured to show the cell outline. **e,** Dark-field image showing the nanowire endoscope inserted into the cytoplasm (left panel). Fluorescence image taken after focused UV irradiation (325 nm, 1 min) on the nanowire tip, showing the QD fluorescence in the cell cytoplasm region under 442 nm laser excitation (right panel). Dark field illumination was left on when the fluorescent image was captured to show the cell outline. Insets in (**d**) and (**e**) are dark-field images of the two cells when the 442 nm excitation laser was turned off, respectively. A 532 nm long-pass filter was used to screen the excitation laser for the fluorescent imaging. The magnifications for (**d**) and (**e**) are the same. **f,** Fluorescence confocal image of a Hela cell after QD delivery showing nanoprobe delivered QDs (red dot) sitting in the cytoplasm within the cell membrane (green), which was labeled with Alexa Fluor® 488 conjugate of wheat germ agglutinin (WGA). 488 nm laser was used to excite both the cell membrane stain and the QDs. Inset is a dark-field image of the cell during QD delivery with a nanowire endoscope. Scale bars in **c**, **e** and **f** are 20 μm.

Figure 3 | Subcellular imaging with nanowire endoscopes in a single living cell. a, Schematic of the subcellular imaging of QDs in a living cell using a nanowire endoscope. **b and c,** Dark field (left panel) and QD fluorescence images (middle and right panel) (**b**) showing the imaging of two adjacent clusters of QDs by a focused 442 nm HeCd laser (middle panel) and endoscope illumination (right panel) through the same laser waveguided through the probe. In the middle and left panel, the dark-field illumination was left on to show the outline of the cell. Each cluster of QDs was delivered into the cell using the photoactive nanowire endoscope as described in Figure 3. The two QD-clusters were located very close to each other (~2 μm apart) and the highly localized illumination from the nanowire endoscope was able to image each of them separately. Fluorescence images (**c**) of QDs showing the spatial resolution of the local illumination by the nanowire endoscope. **d,** Fluorescence image of a live Hela cell, labeled with cell membrane stain, Alexa Fluor® 488 conjugate of WGA, illuminated through wide field 442 nm excitation. **e-f,** Dark field (**e**) and fluorescent (**f**) images of the same cell shown in (**d**) illuminated by a nanowire endoscope (λ = 442 nm).

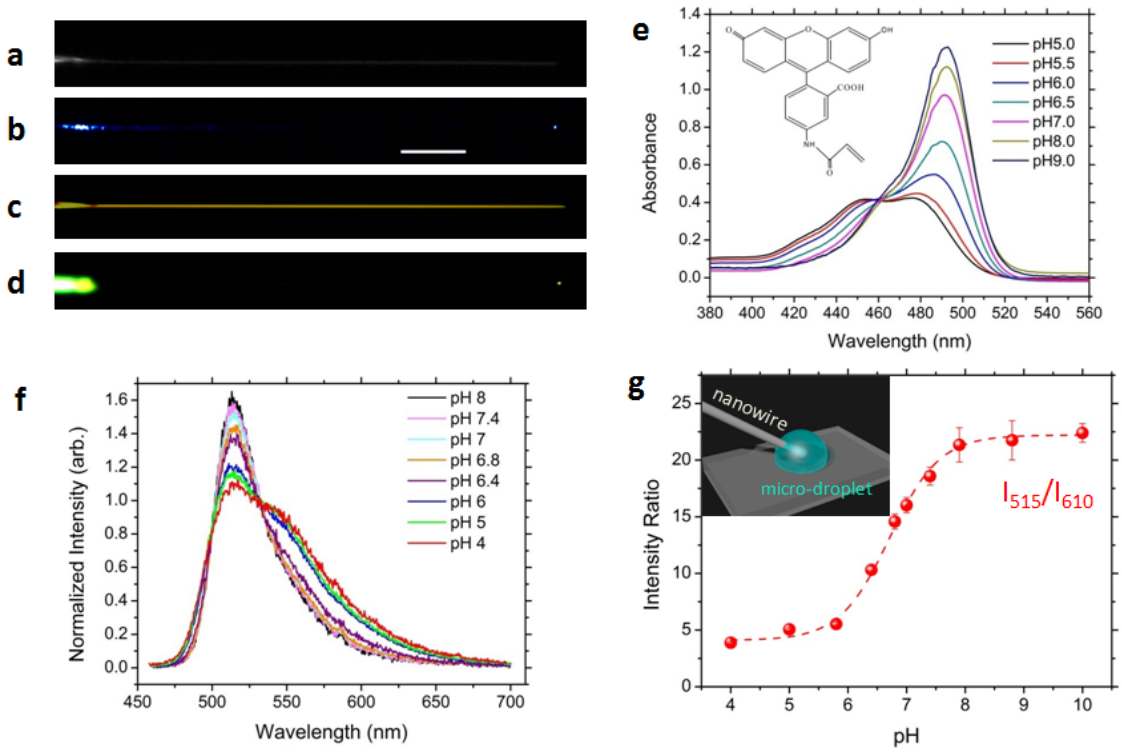

Figure 4. | Local sensing of pH by a nanowire endoscope. a, Dark-field image of a nanowire endoscope before the coating of pH sensitive fluorescent polymer. **b**, Color digital image of blue laser (442 nm) waveguided on the nanowire endoscope. **c**, Dark-field image of the nanowire endoscope after polymer coating. **d**, Color digital images of the nanowire endoscope fluorescence by the blue light waveguided on it after the polymer coating embedded with pH-sensitive dyes. Scare bar is 5 μm. **e**, UV-Vis absorption spectra of N-fluorescein acrylamide (FLAC), the pH sensitive fluorescent dye in buffer solutions of different pH. Inset: molecular structure of FLAC in its protonated form. **f,** Normalized probe tip fluorescence spectra in buffer solutions of different pH. **g**, Calibration curve of the dye-coated nanowire endoscope in a microdroplet containing buffer solution at different pH. Inset: schematic showing the measurement set-up with the nanowire tip immersed in the mircrodroplet of buffer solution.

Figure 5 | Near-field collection of quantum dot (QD) fluorescence in a single living HeLa cell. a, Schematic of the QD fluorescence local detection in a living cell using a nanowire endoscope. The endoscope was placed near the QD (λ_{em}=655nm) that was pre-loaded in the cytoplasm and excited by a blue laser beam. The QD fluorescence was locally collected through the nanowire endoscope which was coupled to a spectrometer. **b,** Dark-field/fluorescence image of a nanowire endoscope placed close to a QD cluster in the cytoplasm that was excited by a focused laser beam (442 nm). **c,** Spectrum of the QD fluorescence collected through the endoscope, showing a single peak centered at ~655nm. **d,** Dark-field/fluorescence images of a nanowire endoscope in close contact with a QD cluster in a HeLa cell (left panel), separated vertically by 2 μm (middle panel) and horizontally by 6 μm from the QD cluster (right panel). The colored circles mark the position of the QD cluster and the tip of the nanowire. The colored arrows in the middle and right panels indicate the endoscope movement with respect to its position in the left panel. **e,** Spectra of QD fluorescence collected through the endoscope corresponding to the 3 images in D respectively. The QD signal faded out fast as the endoscope was moved from the QD cluster. A 532 nm long-pass filter was used to screen the excitation laser for the fluorescent imaging. Scale Bars=50 μm.

Acknowledgements: This work was supported by the Director, Office of Science, Office of Basic Energy Sciences, Material Sciences and Engineering Division, of the U.S. Department of Energy under Contract No. DE-AC02-05CH11231. We thank the National Center for Electron Microscopy for the use of their facilities.